VO^{2+}(IV) Complexes with Pyruvate Carboxylase: Activation of Oxaloacetate Decarboxylation and EPR Properties of Enzyme−VO^{2+} Complexes†

Brian G. Werneburg‡ and David E. Ash*

Department of Biochemistry, Temple University School of Medicine, Philadelphia, Pennsylvania 19140

Received May 29, 1997; Revised Manuscript Received September 8, 1997⊗

ABSTRACT: Chicken liver pyruvate carboxylase catalyzes a nonclassical ping-pong mechanism in which the carboxylation of biotin at subsite 1 of the active site is coupled to the biotin-dependent carboxylation of pyruvate at subsite 2. The functions of two divalent cation cofactors and at least one monovalent cation cofactor in catalysis are not well understood. The oxyvanadyl cation, VO^{2+}, does not support phosphoryl transfer at the first subsite, and uncouples the decarboxylation of oxaloacetate at subsite 2 from the formation of ATP at subsite 1. Stimulation of this oxaloacetate decarboxylase activity in the presence of substrates and cofactors of the first subsite, including VO^{2+}, $VOADP^-$, P_i, and acetyl CoA, suggests that these cofactors and substrates induce the movement of carboxybiotin from the second subsite to the first subsite, where it is decarboxylated. VO^{2+} EPR has provided evidence for enzymic and nucleotide divalent cation binding sites within the first subsite. The EPR properties of enzyme bound VO^{2+} were altered by bicarbonate, suggesting that this substrate ligands directly to VO^{2+} at the enzymic metal site. Fluorescence quenching experiments suggest that a monovalent cation may interact with bicarbonate at the first subsite as well. The results of this study provide evidence that (i) the extrinsic metal ion cofactors interact with the substrates at the first subsite, and that (ii) divalent cations play a role in coupling catalysis at the two nonoverlapping subsites by inducing the decarboxylation of carboxybiotin at the first subsite.

Class I biotin-dependent carboxylases utilize ATP, divalent cations, and bicarbonate to carboxylate biotin, a mobile group that transfers a CO_2 molecule to acceptors such as pyruvate, CoASAc[1], geranyl-CoA, β-methylcrotonyl-CoA, propionyl-CoA, or urea (reviewed by Knowles, 1989). The striking similarities between the reactions catalyzed by this class of enzymes suggest that their mechanisms of catalysis are closely related. Chicken liver pyruvate carboxylase is a tetrameric manganoprotein (Scrutton *et al.*, 1966) that catalyzes the carboxylation of pyruvate to form oxaloacetate (eq 1). Initial velocity studies and product inhibition patterns for this Class I biotin-dependent carboxylase are indicative

$$\text{pyruvate} + \text{ATP} + HCO_3^- \rightleftharpoons \text{oxaloacetate} + \text{ADP} + P_i \quad (1)$$

of a nonclassical bi bi uni uni ping-pong mechanism in which the active site is divided into two nonoverlapping subsites (Barden *et al.*, 1972). The carboxylation of biotin at subsite 1 (reaction 1a) proceeds via the formation of a putative carboxyphosphate intermediate (Wallace *et al.*, 1985; Phillips *et al*., 1992; Attwood, 1993) in a reaction that is activated by CoASAc (Phillips *et al*., 1992). Transfer of CO_2 from carboxybiotin (CO_2-biotin) to pyruvate occurs at subsite 2 (reaction 1b). This nonclassical ping-pong mechanism has characteristics of both ping-pong and sequential kinetics.

$$\text{E-biotin} + \text{MgATP} + HCO_3^- \xrightleftharpoons{\text{CoASAc, } Mg^{2+}, K^+} \text{E-biotin-}CO_2 + \text{MgADP} + P_i \quad (1a)$$

$$\text{E-biotin-}CO_2 + \text{pyruvate} \rightleftharpoons \text{E-biotin} + \text{oxaloacetate} \quad (1b)$$

Significant isotope exchange rates have been observed between $^{32}P_i$/ATP and 2-[^{14}C]-pyruvate/oxaloacetate in the absence of substrates of the sister subsite (Scrutton *et al*., 1965). These exchange rates, as well as the parallel lines observed in plots of 1/v *vs* 1/[ATP] or 1/[bicarbonate] at fixed pyruvate concentrations (up to 3 mM) (Barden *et al*., 1972), are diagnostic of a ping-pong mechanism where product(s) are released before all of the substrate(s) have bound. At higher concentrations of pyruvate, the kinetics become more complicated; Barden *et al.* (1972) have noted that at pyruvate concentrations above 3 mM the lines of the double reciprocal plot display downward curvature. This behavior is indicative of a sequential mechanism where product(s) are not released until all of the substrates have bound. Double reciprocal plots of the velocity of pyruvate carboxylation by the rat liver enzyme, with ATP or bicarbonate as the varied substrate, also give parallel lines at low concentrations of pyruvate and intersecting lines at high pyruvate concentrations. These results at high pyruvate concentrations are indicative of sequential binding of the three substrates (McClure *et al*., 1971a). The kinetic data imply that pyruvate can bind to the second subsite before or after ADP and P_i are released as products from the first subsite. Thus, the two subsites appear to be completely independent, linked only by the mobile biotin arm.

The transfer of CO_2 between the separate and independent subsites by biotin must be controlled in order to efficiently couple the partial reactions in both directions. In both the forward and reverse directions, pyruvate carboxylase drives a thermodynamically unfavorable reaction with a favorable

† This work was supported in part by National Institutes of Health Grant GM 36604.

* Address correspondence to: David E. Ash, Department of Biochemistry, Temple University School of Medicine, 3420 N. Broad St., Philadelphia, PA 19140. Phone: (215)707-4165. Fax: (215)707-7536. Email: deash@astro.ocis.temple.edu.

‡ Supported by a federal work-study award. Present address: Biopolymer Facility, Ohio State University, Columbus, Ohio 43210.

⊗ Abstract published in *Advance ACS Abstracts,* November 1, 1997.

[1] Abbreviations: CoASAc, acetyl-coenzyme A; Hepes, 4-(2-hydroxyethyl)-1-piperazineethanesulfonic acid.

S0006-2960(97)01282-8 CCC: $14.00

one. In the direction of oxaloacetate formation, the cleavage of a high energy phosphoanhydride bond of ATP is coupled to the highly endergonic carboxylation of pyruvate. In the reverse direction, the decarboxylation of oxaloacetate, a highly exergonic reaction, is coupled to the formation of a phosphoanhydride bond between ADP and P_i. In order for partial reactions 1a and 1b to be coupled, the mobile biotin arm must transfer a carboxyl group from the donor subsite to the acceptor subsite after the acceptor has bound. If the CO_2 molecule is transferred to a vacant subsite and released from biotin, it may diffuse from the subsite or react with water to form bicarbonate before an acceptor molecule can bind and react (Easterbrook-Smith *et al*., 1976; Keech & Attwood, 1985; Knowles, 1989).

Identical initial rates for the formation of phosphate (produced at subsite 1) and oxaloacetate (produced at substite 2) are observed for sheep liver pyruvate carboxylase in the forward direction at saturating concentrations of pyruvate. However, at subsaturating concentrations of pyruvate, the rate of oxaloacetate formation is less than the rate of phosphate formation (Easterbrook-Smith *et al*., 1976, Keech & Attwood, 1985; Knowles, 1989). Pyruvate binding at the second subsite is thought to trigger the movement of CO_2-biotin to this site; however, at subsaturating concentrations, pyruvate is thought to dissociate before the arrival of CO_2-biotin, resulting in the formation of HCO_3^- (the "hydrolytic leak") (Easterbrook-Smith *et al*., 1976). Oxamate, an analogue of enolpyruvate, stimulates the rate of oxaloacetate decarboxylation, uncoupled from ATP formation, presumably by inducing the translocation of CO_2-biotin back to subsite 2, where CO_2 is released (Goodall *et al*., 1981; Attwood & Cleland, 1986). Thus, there is strong evidence that the binding of an acceptor molecule in subsite 2 induces the decarboxylation of CO_2-biotin. Our study presents the first evidence indicating that the binding of substrates and metal ion cofactors of the first subsite (VO^{2+}, $VOADP^-$, and P_i) induces the decarboxylation of CO_2-biotin at this site as well.

The roles of at least three divalent cations and one monovalent cation in catalysis are not well understood. An intrinsic Mn^{2+} ion at the second subsite is required for activity but does not appear to provide a catalytic advantage by binding directly to pyruvate (Reed & Scrutton, 1974). Removal of Mn^{2+} with 1,10-phenanthroline results in only a 61% decrease in the 2-[^{14}C]-pyruvate/oxaloacetate exchange rate, suggesting that the intrinsic divalent cation does not have a direct role in catalysis at the second subsite (Carver *et al*., 1988). Rather, a loss of the tetrameric structure of the enzyme upon chelation of Mn^{2+} by 1,10-phenanthroline provides evidence for a structural role for the intrinsic metal (Carver *et al*., 1988).

At least two extrinsic divalent cations, including the divalent cation associated with the nucleotide, are required for maximal catalytic activity (Barden & Scrutton, 1974). Steady-state kinetic analysis indicates that Mg^{2+} and $MgATP^{2-}$ bind randomly, but synergistically, to the enzyme (Barden & Scrutton, 1974). Direct physical evidence for two extrinsic divalent cation binding sites has been provided by EPR spectroscopy, which showed that extrinsic Mn^{2+} binds to pyruvate carboxylase in the presence of the substitution inert $CrATP^-$ metal−nucleotide complex (Reed & Scrutton, 1974). In the present study $^{51}VO^{2+}$ ($S = {}^1/_2$; $I = {}^7/_2$) was used to probe for interactions between substrates and the enzymic and nucleotide divalent cations. The VO^{2+} EPR results indicate that VO^{2+} and $VOATP^{2-}$ bind in a random fashion and suggest that bicarbonate interacts with the enzymic VO^{2+} at subsite 1.

Monovalent ions, including K^+, NH_4^+, Rb^+, Cs^+, and Tl^+, afford a 3−7 fold activation of the catalytic rate (Barden & Scrutton, 1974). Steady-state kinetic analysis indicates that K^+ and HCO_3^- bind in an equilibrium-ordered fashion, with bicarbonate adding first, and it has been proposed that the binding of the monovalent cation serves to trap bicarbonate at the active site (Barden & Scrutton, 1974). However, the monovalent cation site has not been characterized, and the function of the monovalent cation in catalysis is unknown. Our data indicate that bicarbonate enhances the binding of the monovalent cation and suggest that there is at least one monovalent cation binding site in subsite 1.

MATERIALS AND METHODS

Materials. Glucose-6-phosphate dehydrogenase, hexokinase, lactate dehydrogenase, and malate dehydrogenase were purchased from Sigma Chemical Co. Fresh chicken livers were obtained from Tyson Foods, New Holland, Pa. Chelex-100 was purchased from Bio-Rad. D_2O (99.8%) was purchased from Aldrich Chemical Co. $VOSO_4$ was obtained from Alfa Inorganics, and the concentrations of $VOSO_4$ solutions were determined by absorbance at 750 nm with an extinction coefficient of 18 M^{-1} cm^{-1} (Fitzgerald & Chasteen, 1974). γ-F-ATP was kindly provided by Dr. George D. Markham. The $(CH_3)_4N^+$ salt of pyruvate was prepared by neutralizing pyruvic acid with tetramethylammonium hydroxide, and the $(CH_3)_4N^+$ salt of HCO_3^- was prepared by bubbling CO_2 gas into a solution of 1 M $(CH_3)_4$-NOH until a pH value of 8 was reached. The $(CH_3)_4N^+$ salts of ADP and CoASAc were prepared by chromatography of the Na^+ and Li^+ salts on a bed of Bio Gel AG50-X8 cation resin charged with $(CH_3)_4N^+$. All other chemicals were of the highest purity commercially available.

Chicken Liver Pyruvate Carboxylase. Pyruvate carboxylase (subunit mw = 130000) was purified from chicken liver as described previously (Werneburg & Ash, 1993). The purified enzyme had specific activities in the range of 17 to 25 units per mg of protein as determined by the standard assay for oxaloacetate formation (Duggelby *et al*., 1982). A unit of activity is defined as the amount of enzyme required to catalyze the production of 1 μmol of oxaloacetate per min at 25 °C. Protein concentrations were determined by absorbance using the extinction coefficient $\epsilon^{0.1\%} = 0.70$ at 280 nm (Scrutton & Fung, 1972). The enzyme was determined to be greater than 90% homogeneous by SDS polyacrylamide gel electrophoresis.

Enzyme Assay. All assays were performed at pH 7.8. The storage buffers of the coupling enzymes were replaced with 100 mM Hepes−KOH at pH 7.8, 50 mM KCl, and 5% glycerol by ultrafiltration. Enzyme activity in the direction of pyruvate carboxylation was measured with the malate dehydrogenase coupled assay described by Duggleby *et al.* (1982). A 1 mL reaction mixture contained 100 mM Hepes−KOH at pH 7.8, 5 mM pyruvate, 2 mM ATP, 5 mM $MgCl_2$, 30 mM $KHCO_3$, 30 μM CoASAc, 80 μM NADH, and 11 units of malate dehydrogenase. Phosphate production in the forward direction was measured with a molybdate reagent that detects nanomole amounts of inorganic phosphate (González-Romo *et al*., 1992). The assay mixture was

similar in composition to that utilized to measure oxaloacetate formation except that NADH and malate dehydrogenase were omitted.

In the reverse direction, the decarboxylation of oxaloacetate linked to the phosphorylation of ADP at the first subsite was coupled to the reduction of pyruvate with lactate dehydrogenase (McClure *et al.*, 1971b). The 1 mL reaction mixture for the continuous assay contained 100 mM Hepes−KOH at pH 7.8, 40 mM K_2HPO_4, 4 mM ADP, 750 μM oxaloacetate, 7.5 mM $MgCl_2$, 160 μM CoASAc, 80 μM NADH, and 13 units of lactate dehydrogenase. The background rate of NADH oxidation observed before the addition of pyruvate carboxylase was subtracted from the rate observed in the presence of the enzyme to yield the rate of catalysis. The production of ATP coupled to the decarboxylation of oxaloacetate was measured in a 1 mL reaction mixture containing 100 mM Hepes−KOH at pH 7.8, 40 mM K_2HPO_4, 2 mM ADP, 750 μM oxaloacetate, 160 μM CoASAc, and 5 mM $MgSO_4$. The amount of ATP produced was determined with a coupled hexokinase/glucose 6-phosphate dehydrogenase assay mixture containing 500 μM glucose, 160 μM $NADP^+$, 1 unit of hexokinase, and 5 units of glucose 6-phosphate dehydrogenase.

ATP formation from ADP and carbamoyl phosphate was also measured using a hexokinase/glucose 6-phosphate dehydrogenase coupled assay (Attwood & Graneri, 1991). The 1 mL reaction mixture contained 2 mM ADP, 20 mM carbamoyl phosphate, 250 μM CoASAc, and 7.5 mM $MgCl_2$. The rate of ATP formation was determined as described above by end-point assay with 500 μM glucose, 500 μM $NADP^+$, 1 unit of hexokinase, and 5 units of glucose-6-phosphate dehydrogenase.

Oxaloacetate decarboxylation uncoupled from ATP formation at the first subsite can occur under two conditions. In the reaction mixture described for oxaloacetate decarboxylation linked to ATP formation, oxaloacetate decarboxylation and ATP formation are uncoupled when 600 μM VO^{2+} and 300 μM ADP replace 7.5 mM Mg^{2+} and 2 mM ADP. Oxaloacetate can also be decarboxylated in the absence of any added nucleotide substrate. This activity, which is stimulated by oxamate, was measured with a lactate dehydrogenase coupled assay containing 500 μM oxaloacetate, 60 μM oxamate, 160 μM CoASAc, 80 μM NADH, and 11 units of lactate dehydrogenase (Attwood & Cleland, 1986). The enzyme catalyzed rates were corrected for changes in absorbance at 340 nm due to the presence of VO^{2+} and to uncatalyzed oxaloacetate decarboxylation. Aggregation of VO^{2+} in Hepes buffer (Chasteen, 1981) may have caused the observed time-dependent increase in absorbance at 340 nm. The enzyme was assayed for activity shortly after the addition of VO^{2+} to the reaction mixture to minimize complications arising from vanadyl aggregation.

Metal Ion Activation. Pyruvate carboxylase stored in 25 mM potassium phosphate at pH 7.2, 1.5 M sucrose, 1 mM EDTA, and 5 μM phenylmethyl sulfonyl fluoride was dialyzed against 100 mM Hepes−KOH at pH 7.8 containing 50 mM KCl, 6−8% glycerol, and 1 mM dithiothreitol or dithioerythritol. The enzyme typically retained 80% of its original activity. The presence of a reducing agent was required to prevent oxidation of V(IV) to V(V) (Chasteen, 1981). Phosphate and oxaloacetate production were measured under conditions similar to those described under "Enzyme Assay" except that 600 μM $VOSO_4$ and 300 μM ATP or 5 mM $MgSO_4$ and 2 mM ATP were used. In the reverse direction, the formation of pyruvate and ATP was assayed as described under "Enzyme Assay" except that 600 μM $VOSO_4$ and 300 μM ADP or 7.5 mM $MgSO_4$ and 2−4 mM ADP were used. ATP formation from carbamoyl phosphate and ADP was measured with 600 μM $VOSO_4$ and 300 μM ADP or 7.5 mM $MgSO_4$ and 2 mM ADP. Oxamate-induced oxaloacetate decarboxylation was assayed in the presence of 600 μM $VOSO_4$ or 7.5 mM $MgSO_4$. The catalytic rates were corrected for changes in absorbance at 340 nm due to VO^{2+} aggregation and uncatalyzed oxaloacetate decarboxylation (for assays in the reverse direction) as described earlier.

Pyruvate carboxylase used in the monovalent cation activation assay was dialyzed against 100 mM Hepes−$(CH_3)_4NOH$ at pH 7.8 containing 6% glycerol. Following this procedure the enzyme retained 60% of its original activity. Pyruvate carboxylase was assayed in 100 mM Hepes−$(CH_3)_4NOH$ at pH 7.8 containing 5 mM tetramethylammonium pyruvate, 2 mM monoethanolammonium ATP, 30 mM tetramethylammonium bicarbonate, 30 μM tetramethylammonium CoASAc, 5 mM $MgSO_4$, the nitrate salt of either thallium or potassium, 80 μM NADH, and 11 units of malate dehydrogenase. The storage buffer for the coupling enzyme was replaced with 100 mM Hepes−$(CH_3)_4NOH$ at pH 7.8 containing 6% glycerol by centrifugation at 4300*g* in 30000 molecular weight cutoff Amicon Centricon microconcentrators. Double reciprocal plots were generated using tetramethylammonium nitrate to maintain constant ionic strength and nitrate concentration.

Intrinsic Fluorescence Quenching by the Metal Ions. Pyruvate carboxylase exhibits intrinsic protein fluorescence with an emission maximum of 337 nm upon excitation at 294 nm, the excitation maximum. Upon binding divalent cations, the intrinsic fluorescence of the protein was quenched. Fluorescence spectra were recorded at 25 °C (excitation and emission slit widths set for 5 nm band pass) with a Perkin-Elmer 650-10S fluorescence spectrophotometer. The storage buffer for the enzyme was first replaced with buffer that had been batch treated with Chelex-100 in the sodium form to remove divalent cations. Enzyme used in the Mg^{2+} and Mn^{2+} titrations was dialyzed against 100 mM Hepes−KOH at pH 7.8 containing 50 mM KCl and 10% glycerol. Enzyme used in the VO^{2+} titration was dialyzed against the same buffer with 1 mM dithiothreitol or dithioerythritol. Monovalent cation binding was monitored by fluorescence spectroscopy using enzyme that had been dialyzed against 100 mM Hepes−$(CH_3)_4NOH$ at pH 7.8 containing 6% glycerol and 1 mM β-mercaptoethanol.

VO^{2+} EPR Spectroscopy. $^{51}VO^{2+}$ ($S = {}^1/_2$; $I = {}^7/_2$) was used as a spectroscopic probe of two divalent cation binding sites on pyruvate carboxylase. VO^{2+} is the most stable oxycation of the first row transition metals (Chasteen, 1981), forming complexes that are pentacoordinate or square bipyramidal with a short V=O bond. The complexes formed are similar to Mg^{2+} complexes that are usually hexacoordinate in nature. VO^{2+} is useful as a spectroscopic probe because it forms anionic, cationic, and neutral complexes with all types of ligands, and because it is EPR silent in water in the absence of chelators. The effective magnetic moment of the unpaired electron of the ^{51}V isotope (100% natural abundance) has axial symmetry; the components of the magnetic moment are $g_{\parallel}\beta_e/2$ and $g_{\perp}\beta_e/2$. Physical

effects on the magnetic environment of the unpaired electron, including those caused by equatorial ligand substitution in the first coordination sphere of VO^{2+}, are embodied in the anisotropic g factor ($g\|$, $g\perp$) and ^{51}V hyperfine coupling constant ($A\|$, $A\perp$). VO^{2+} bound to small molecules such as HCO_3^- and ATP gives rise to isotropic eight line patterns at room temperature due to hyperfine interaction between the electron spin and the nuclear spin. VO^{2+}−protein complexes do not give rise to isotropic eight line patterns in solution; they exhibit anisotropic 16 line powder spectra due to the long rotational correlation times of the protein. The powder spectra are comprised of transitions from spin states that are parallel and perpendicular (symmetry axis along the V═O bond) to H_o (Chasteen, 1981; Markham, 1984).

Pyruvate carboxylase was prepared for EPR by dialysis against 100 mM Hepes−KOH at pH 7.8, 50 mM KCl, 6% glycerol, and 1 mM dithiothreitol or dithioerythritol. The enzyme was concentrated to 110−130 mg/mL by centrifugation at 4300*g* in 30000 molecular weight cutoff Centricon concentrators. The final concentration of pyruvate carboxylase, which retained 80% of its original activity, was 700−900 μM enzyme subunit in the EPR samples. In preparation for EPR experiments utilizing D_2O, pyruvate carboxylase was dialyzed against 100 mM Hepes−KOH at pH 7.8, 50 mM KCl, 6% glycerol, and 1 mM dithioerythritol. In separate vials, two 100 mL aliquots of 100 mM Hepes−KOH at pH 7.8, 50 mM KCl, and 1 mM dithioerythritol were lyophilized; one of the buffers was dissolved in H_2O and 6% glycerol while the other was dissolved in D_2O and 6% glycerol, which contained deuterium at the exchangeable proton positions. Exchangeable protons on glycerol were replaced with deuterium by three rounds of rotoevaporation and D_2O addition to remove H_2O. Protonated and deuterated enzyme samples were prepared by dialysis against the two buffers and concentrated to 110−130 mg/mL by ultrafiltration in 30000 molecular weight cutoff Centricons at 4300*g*. Where appropriate, solutions of CoASAc, ATP, and $VOSO_4$ were prepared by dissolving lyophilized stock solutions in D_2O.

EPR spectra were recorded at 9.4 GHz with a Bruker ESR 200D spectrometer. 4-Hydroxy-2,2,6,6-tetramethylpiperidinyl-1-oxy ($g = 2.006$) was used as a g-value standard. The powder spectra are reported as the sum of 4 scans. The spectra of protein bound vanadyl species were corrected for contributions from nonenzymic complexes of VO^{2+} with glycerol, CoASAc, nucleotide, and bicarbonate by spectral subtraction.

Tl^+−VO^{2+} Superhyperfine Coupling. Thallous ion (^{203}Tl, $I = {}^1/_2$, 29.52% natural abundance; ^{205}Tl, $I = {}^1/_2$, 70.48% natural abundance) was used as a spin probe of the monovalent cation binding site(s). Superhyperfine coupling between the electron spin of protein bound VO^{2+} and the nuclear spin of Tl^+ provides direct evidence for the proximity of the two cations. The magnetic moments of the two thallium isotopes are too similar to observe distinct superhyperfine coupling from the two isotopes. This superhyperfine interaction may occur via through-space superhyperfine coupling between VO^{2+} and Tl^+ or via through-bond coupling, which occurs when the electron spin is delocalized into ligand orbitals with S character (Lord & Reed, 1987; Markham & Leyh, 1987). Through-bond coupling occurs when VO^{2+} and Tl^+ share a first coordination sphere ligand, providing a path for electron spin delocalization. The parallel and perpindicular lines of an axially symmetric vanadyl species are split by equal magnitude as a result of through bond superhyperfine coupling. In contrast, through space superhyperfine coupling between thallium and an axially symmetric vanadyl magnetic moment will split the parallel and perpindicular hyperfine lines by different magnitudes.

To test for such superhyperfine interaction, pyruvate carboxylase was prepared by dialysis against 100 mM Hepes−$(CH_3)_4NOH$ at pH 7.8 containing 6% glycerol and 1 mM dithiothreitol. The protein was concentrated to 130 mg/mL by centrifugation at 4300*g* in 30000 molecular weight cutoff Centricon concentrators and retained 60% of its original activity following this procedure. Thallium nitrate was added to the protein samples at the indicated concentrations. Spectra were accumulated as described under "VO^{2+} EPR Spectroscopy" and compared to spectra obtained for identical samples in the absence of Tl^+.

Simulation of the VO^{2+} EPR Spectra. The powder spectra of the protein bound species were simulated to determine the magnitudes of the ^{51}V hyperfine coupling constants and g values using the VO^{2+} EPR simulation program QPOW (Nilges, 1979; Belford and Nilges, 1979; Maurice, 1982). QPOW simulates the powder spectrum of an $S = {}^1/_2$ system with one hyperfine nucleus and up to three superhyperfine nuclei. Multiple iterations of the spectral parameters were made to produce simulated spectra that best fit the experimental spectra in terms of the positions and widths of the resonance lines.

Table 1: Divalent Cation Activation of Pyruvate Carboxylase[a]

	activity (units/mg)		
product formation	Mg^{2+}	VO^{2+}	no metal
oxaloacetate (forward direction)	12.9[b]	$<1 \times 10^{-3}$	$<1 \times 10^{-3}$
phosphate (forward direction)	13.1[b]	$<1 \times 10^{-3}$	$<1 \times 10^{-3}$
pyruvate (reverse direction)	0.75	0.26	9.2×10^{-3}
ATP (reverse direction)	0.65[c]	$<1 \times 10^{-3}$	$<1 \times 10^{-3}$
ATP (from $H_2NCOPO_4^{2-}$)	1.7×10^{-2}	$<1 \times 10^{-3}$	3.4×10^{-3}
pyruvate[d] (oxamate induced)	9.0×10^{-2}	9.7×10^{-2}	0.1

[a] Assays for product formation in the forward and reverse directions as described under "Materials and Methods" were made using 7.5 mM $MgSO_4$ and 2 mM ADP or ATP; 600 μM $VOSO_4$ and 300 μM ADP or ATP; or no metal and 2 mM ADP or ATP except where noted. Pyruvate carboxylase was prepared for assay as described under "Materials and Methods". [b] 5 mM $MgSO_4$. [c] 4 mM ADP. [d] No nucleotide was added.

RESULTS

Divalent Cation Activation. The oxycation of vanadium, VO^{2+}, does not activate the pyruvate carboxylase reaction in the forward direction as measured by assays for P_i or oxaloacetate (Table 1). However, in the reverse direction, VO^{2+} stimulated the decarboxylation of oxaloacetate to a rate that was 30% of that for the decarboxylation of oxaloacetate linked to the phosphorylation of ADP at subsite 1 in the presence of Mg^{2+}. Although VO^{2+} supported oxaloacetate decarboxylation, no ATP production was measured under these conditions, indicating that the decarbox-

Table 2: Oxaloacetate Decarboxylation Uncoupled from ATP Formation[a]

cofactors	activity (units/mg)
160 μM CoASAc, 300 μM ADP, 40 mM P_i	0.17
160 μM CoASAc, 300 μM ADP	0.02
160 μM CoASAc, 40 mM P_i	0.01
160 μM CoASAc	0.003
300 μM ADP, 40 mM P_i	0.01
160 μM CoASAc, 300 μM ATP, 30 mM HCO_3^-	0.02

[a] Pyruvate carboxylase was prepared and assayed for pyruvate formation in the presence of 600 μM $VOSO_4$ as described under "Materials and Methods".

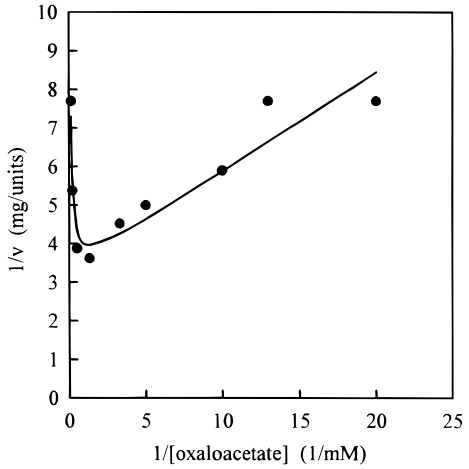

FIGURE 1: Reciprocal plot of the VO^{2+}, ADP, P_i, CoASAc-induced oxaloacetate decarboxylase activity. Pyruvate carboxylase was prepared and assayed as described under "Materials and Methods". The data were fit to eq 2.

ylation of oxaloacetate was uncoupled from ATP formation at subsite 1. In addition, no ATP formation was detected from ADP and carbamoyl phosphate, an analogue of carboxyphosphate, in the presence of VO^{2+}. Although VO^{2+} did not support phosphoryl transfer at subsite 1, CoASAc and the two substrates that bind to subsite 1, ADP and P_i, were required for a maximal rate of oxaloacetate decarboxylation in the presence of VO^{2+}, suggesting that subsite 1 was involved in this reaction (Table 2).

The VO^{2+}, ADP, P_i, and CoASAc-induced decarboxylation of oxaloacetate was treated as a single substrate reaction with VO^{2+}, ADP, P_i, and CoASAc acting as activators. The concentration of VO^{2+} required for half maximal activation (210 $\pm$ 80 μM) was determined under steady-state conditions. The K_m for oxaloacetate (80 $\pm$ 21 μM) was determined from a fit of the data to eq 2 (Figure 1), which describes substrate inhibition resulting from a dead-end complex of substrate with the incorrect form of the enzyme (Cleland, 1970). Substrate inhibition was evident only at high concentrations of oxaloacetate; analysis of the data in Figure 1 yielded a K_i of 6.4 $\pm$ 1.9 mM.

$$1/v = 1/V_{max} + [S]/K_i V_{max} + K_m/V_{max}[S] \qquad (2)$$

Intrinsic Fluorescence Quenching by the Divalent Cations. Pyruvate carboxylase exhibited intrinsic protein fluorescence with an emission maximum of 337 nm upon excitation at 294 nm. The intrinsic fluorescence of the enzyme was quenched upon the addition of Mg^{2+}, Mn^{2+}, or VO^{2+} (Table 3). The absolute decrease in fluorescence, *q*, was plotted *versus* cation concentration, and the dissociation constants

Table 3: Dissociation Constants of the Divalent Cation−Pyruvate Carboxylase Complexes[a]

	Q (maximum quench, arbitrary units)	K_d (μM)	n_{app}
Mg^{2+}	1.0	4700 $\pm$ 2100	0.5 $\pm$ 0.2
Mn^{2+}	1.5	93 $\pm$ 20	0.98 $\pm$ 0.23
VO^{2+}	50.0	155 $\pm$ 10	1.06 $\pm$ 0.03

[a] Pyruvate carboxylase was prepared as described under "Materials and Methods." The intrinsic protein fluorescence (excitation maximum = 294 nm; emission maximum = 337 nm) of pyruvate carboxylase, 10 μM enzyme subunit concentration, was quenched with the divalent cations and the titration curves were fit to eq 3.

for the metal−enzyme complexes were determined by fitting the data to the Hill equation (eq 3), where *Q* is the maximum quench and *K′* is a constant comprised of the intrinsic dissociation constant, K_d, and the factors by which ligand binding affects the dissociation constant (Segel, 1975). *K′* reduces to the intrinsic dissociation constant when *n* is 1.

$$q = Q[L]^n/([L]^n + K') \qquad (3)$$

$$K' = K_d n(a^{n-1}b^{n-2}c^{n-3}...z^1)$$

VO^{2+} caused the greatest reduction in intrinsic fluorescence while binding noncooperatively to pyruvate carboxylase, with a K_d = 155 $\pm$ 10 μM. The apparent *n* value of 1 for VO^{2+} is the minimum number of binding sites (Segel, 1975). Mg^{2+} bound less tightly than the transition metal ions, and there were large uncertainties in K_d and n_{app}.

VO^{2+} EPR of the Divalent Cation Binding Sites. The EPR signal for the VO^{2+}−enzyme complex in solution was characteristic of a 16 line powder type spectrum due to the long rotational correlation time of the protein. The spectrum for a frozen sample recorded at 173 K (Figure 2) was slightly sharper than the solution spectrum observed at 273 K. Because only bound VO^{2+} gave rise to a VO^{2+} powder spectrum, the concentration of bound VO^{2+} was proportional to the amplitude of the EPR signal. When the sum of the amplitudes of the $-5/2||$ and $-7/2||$ transition peaks was plotted *versus* VO^{2+}/enzyme subunit, the stoichiometry of binding of VO^{2+} to the enzyme was found to be 1 per enzyme subunit (Figure 3). This VO^{2+} EPR signal observed at a concentration of 1 mM VO^{2+} could not be reduced by the addition of up to 450 mM magnesium, indicating that magnesium does not effectively displace vanadyl cation from this enzymic site. Simulation of the EPR spectrum with QPOW was achieved with *g* values and hyperfine coupling constants listed in Table 4. The *g* values and hyperfine coupling constants of VO^{2+} are sensitive to the equatorial ligands in the first coordination sphere; *A*|| determined by simulation of the enzymic VO^{2+} spectrum was indicative of nitrogenous ligands in the first coordination sphere (Chasteen, 1981; Zhang *et al.*, 1993).

Evidence for a second VO^{2+} binding site, a nucleotide associated site, was obtained upon addition of ATP to a solution of enzyme and excess $VOSO_4$; a second 16 line powder spectrum was observed in addition to the enzymic site spectrum, resulting in a 32 line spectrum in solution at 273 K. Again, the resolution was improved upon freezing the sample at 173 K. The 16 line VO^{2+} spectrum observed prior to the addition of nucleotide was subtracted from the 32 line spectrum obtained in the presence of nucleotide

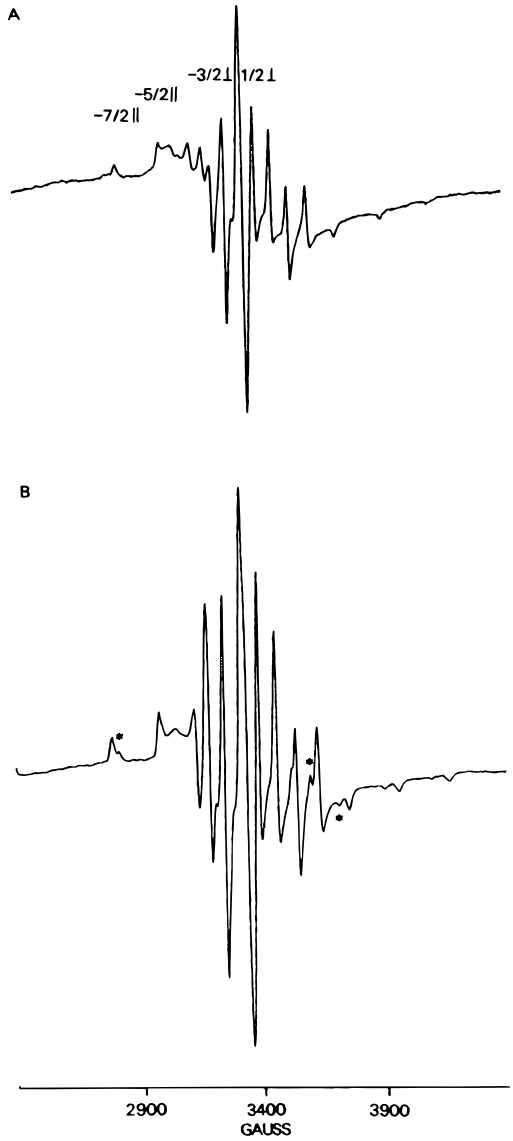

FIGURE 2: EPR spectra of the enzymic and nucleotide VO^{2+} sites. The enzyme was prepared for EPR as described under "Materials and Methods". EPR spectra were recorded at 9.4 GHz and 173 K with a modulation amplitude of 6.3 gauss. Sample A contained 840 μM enzyme subunit, 850 μM $VOSO_4$, and 1.9 mM CoASAc. Sample B contained 750 μM enzyme subunit, 1.4 mM $VOSO_4$, 1.7 mM CoASAc, 3.8 mM ATP. A 32 line spectrum was generated from sample B comprised of signals from the VO^{2+}-enzyme complex designated by *, and the $VOATP^{2-}$-enzyme complex.

(Figure 2) to facilitate studies of the nucleotide-dependent spectrum. After subtraction of the enzymic site powder spectrum, the EPR spectrum for VO^{2+} bound at the nucleotide site was simulated (Table 4). The value of 176.4 $\times$ 10^{-4} cm^{-1} for $A||$, determined by simulation, is indicative of oxygen ligands in the first coordination sphere. When phosphate oxygens ligate to all four equatorial positions of VO^{2+}, the $A||$ is equal to 171 $\times$ 10^{-4} cm^{-1} (Zhang *et al.*, 1993), while $A||$ is equal to 170.9 $\times$ 10^{-4} cm^{-1} when four carboxylate oxygens are ligands, and $A|| = 182.6 \times 10^{-4}$ cm^{-1} when four water oxygens are bound to VO^{2+} (Chasteen, 1981).

ADP, γ-F-ATP, and γ-S-ATP (Figure 4) all bound readily to the nucleotide binding site as indicated by the appearance of the second VO^{2+} spectrum. γ-F-ATP and γ-S-ATP were not substrates in the pyruvate carboxylation reaction in the presence of Mg^{2+}, but the g values and hyperfine coupling

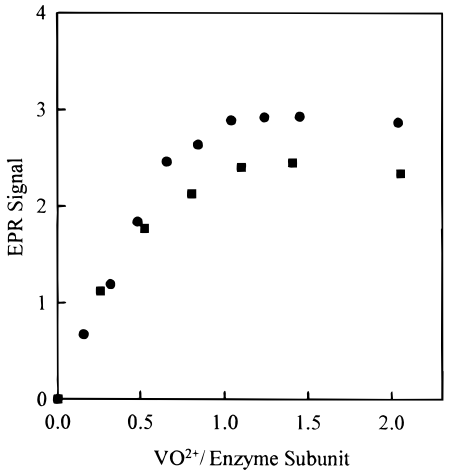

FIGURE 3: Titrations of the enzymic and nucleotide metal binding sites with VO^{2+}. The enzyme was prepared for EPR as described under "Materials and Methods". EPR spectra were recorded at 9.4 GHz and 293 K with a modulation amplitude of 10 gauss. The enzymic site of pyruvate carboxylase, 800 μM enzyme subunit, was titrated with VO^{2+} in the presence of 1.33 mM CoASAc, and the sum of the $-5/2||$ and $-7/2||$ transition peaks was plotted *versus* VO^{2+}/enzyme subunit (■). The nucleotide site was titrated in the presence of 1.29 mM CoASAc, 1.29 mM ATP, and 1 mM $MgSO_4$ (The small amount of Mg^{2+} present did not affect the titration; 1 mM Mg^{2+} displaces neither the enzymic nor the nucleotide VO^{2+}.) The $-7/2||$ peak was plotted *versus* VO^{2+}/enzyme subunit (●).

Table 4: Hyperfine Coupling Constants for VO^{2+} Complexes of Pyruvate Carboxylase[a]

complexes	$g\|\|$	$g\perp$	$A\|\|$ ($cm^{-1} \times 10^4$)	$A\perp$ ($cm^{-1} \times 10^4$)
VO^{2+}−enz	1.943	1.978	163.1	58.7
VO^{2+}−enz−HCO_3^-	1.939	1.979	158.8	57.7
VO^{2+}−ADP−enz	1.929	1.973	174.4	66.4
VO^{2+}−ATP−enz	1.929	1.973	176.4	66.4
VO^{2+}−γ-F-ATP−enz	1.929	1.973	176.1	66.4
VO^{2+}−γ-S-ATP−enz	1.929	1.973	177.1	66.4

[a] Pyruvate carboxylase was prepared for EPR as described under "Materials and Methods". Solution spectra recorded at 9.4 GHz and 293 K, with modulation amplitudes of 6−10 gauss. VO^{2+} EPR spectra were simulated with QPOW (Nilges, 1979; Belford and Nilges, 1979; and Maurice, 1982) to determine the g factors and hyperfine coupling constants. The experimental spectra used for simulation were the sums of four 200 s scans.

constants exhibited in the VO^{2+} powder spectra were similar to those for the powder spectra observed in the presence of ADP and ATP, indicating that the analogues of ATP bound to the nucleotide site (Table 4). Substitution of an oxygen atom at the γ-phosphoryl group of ATP with fluorine or sulfur had little or no effect on the EPR parameters of VO^{2+} bound at the nucleotide site. A distinct difference between the coupling constants of VO^{2+} at the nucleotide site in the presence of ATP and the analogues could have provided direct evidence for a ligand from the gamma phosphoryl group, since sulfur and fluorine would be expected to perturb the coupling constants. However, no such effect was observed.

Saturation of the nucleotide binding site occurred upon the addition of 1 equiv of VO^{2+} per enzyme subunit in the presence of ATP, indicating that the nucleotide site becomes saturated with VO^{2+} before the enzymic site (Figure 3) in the presence of ATP. In order for the nucleotide site to be populated with VO^{2+} before the enzymic site in this experiment, the K_d for the $VOATP^{2-}$-enzyme complex must

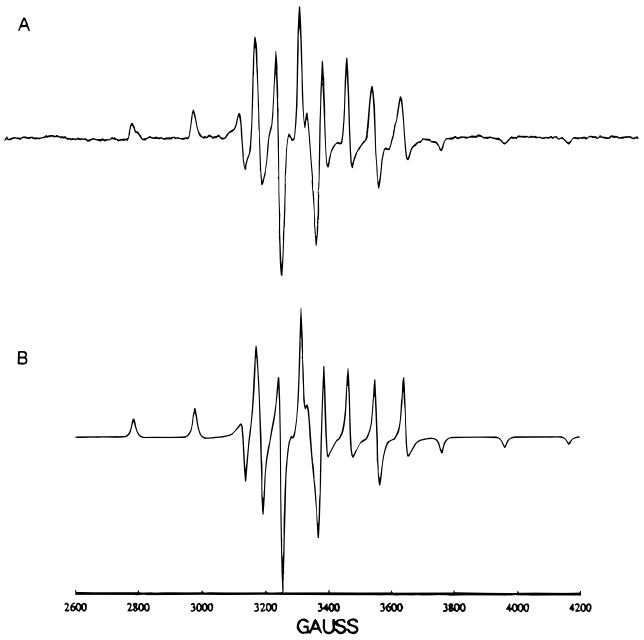

FIGURE 4: EPR spectrum of the $VO^{2+}-\gamma$-S-ATP−enzyme complex. The enzyme was prepared for EPR as described under "Materials and Methods". EPR spectra were recorded at 9.4 GHz and 273 K with a modulation amplitude of 15.8 gauss. Spectrum A was obtained from the difference between the 32 line spectrum observed from a sample containing 852 μM enzyme subunit, 1.92 mM $VOSO_4$, and 4.0 mM γ-S-ATP, and the 16 line spectrum from a sample containing 888 μM enzyme subunit, 2.0 mM $VOSO_4$. Spectrum B is a simulation of spectrum A generated by QPOW (Nilges, 1979; Belford and Nilges, 1979; and Maurice, 1982) with the parameters reported in Table 4.

be lower than that for VO^{2+} binding to the enzymic site (150 μM), or the affinity of the nucleotide for VO^{2+} must be greater than the affinity of the enzymic site for the metal ion. While VO^{2+} and nucleotides form a 1:2 complex in solution (Mustafi *et al.*, 1992), it appears that a 1:1 complex of VO^{2+} and ATP binds at the nucleotide site, as the nucleotide site was 70% saturated after the addition of 1 equiv of ATP. Approximately 90% of the VO^{2+} bound to the nucleotide site could be displaced by 450 mM Mg^{2+}, demonstrating that $VOATP^{2-}$ bound to the same site as $MgATP^{2-}$.

These EPR results also indicate that VO^{2+} and $VOATP^{2-}$ bind randomly to pyruvate carboxylase, since the enzyme−VO^{2+} and the enzyme−$VOATP^{2-}$ complexes are both readily formed. These results agree with the observation of random binding of Mg^{2+} and $MgATP^{2-}$ by kinetic analyses (Barden & Scrutton, 1974).

VO^{2+} EPR of the Enzymic and Nucleotide Binding Sites in D_2O. The sensitivity of the hyperfine coupling constants to the equatorial ligands of VO^{2+} was used to determine the number of ligands with exchangeable protons at the enzymic and nucleotide binding sites. Ligands, such as water molecules, or the ϵ-NH_2 groups of lysine residues (Zhang *et al.*, 1993) can be detected by inhomogeneous broadening of the $+^1/_2\perp$ and $-^3/_2\perp$ spin state transitions of VO^{2+} due to superhyperfine coupling between the electron spin of ^{51}V and the proton nuclear spins. Replacement of one equatorial water ligand with D_2O results in a 1.6 gauss narrowing of the $+^1/_2\perp$ and $-^3/_2\perp$ hyperfine lines (Albanese & Chasteen, 1978; Markham, 1984). The $\perp$ hyperfine lines of the pyruvate carboxylase−VO^{2+} complex in the protonated buffer were broadened by 3.4 gauss compared to those for the same complex prepared in D_2O, indicating that two of the equatorial ligands are H_2O and/or the ϵ-NH_2 group of the lysine side chain (Table 5). The other two equatorial ligands in the enzyme−VO^{2+} complex do not have exchangeable protons and are donated by the protein. The $\perp$ hyperfine lines of VO^{2+} at the $VOATP^{2-}$−enzyme site (Table 5) were broadened only slightly by 0.2 to 1.0 gauss, suggesting that at most one ligand with exchangeable protons is coordinated to VO^{2+}, with three or four of the remaining ligands being donated by nucleotide phosphoryl oxygens and/or the protein.

Table 5: Line Width Narrowing in Deuterium Solvent[a]

	EPR transition	line width (G) H_2O	line width (G) D_2O	H_2O/NH_2 ligands
VO^{2+}−enz	$+1/2\perp$	12.6 ± 0.8	9.2 ± 0.3	2.1 ± 0.5
	$-3/2\perp$	12.2 ± 0.6	8.8 ± 0.4	2.1 ± 0.4
VO^{2+}−ATP−enz	$+1/2\perp$	14.6 ± 0.1	14.4 ± 0.1	0.1 ± 0.1
	$-3/2\perp$	15.1 ± 0.2	14.1 ± 0.2	0.6 ± 0.3

[a] Protonated and deuterated pyruvate carboxylase samples were prepared as described under "Materials and Methods". The spectra were recorded at 9.4 GHz and 200 K with a modulation amplitude of 4 gauss. The peak to peak line widths were determined from the average of 2−4 scans. The concentrations of enzyme, substrates, and cofactors for the binary species were as follows; 710 μM enzyme subunit concentration, 650 μM $VOSO_4$, and 1.5 mM CoASAc. The ternary species was produced in a sample comprised of 670 μM enzyme subunit, 1.2 mM $VOSO_4$, 1.4 mM CoASAc, and 3.5 mM ATP.

Interaction of the Cofactors, Substrates, and Substrate Analogues of the First Partial Reaction with VO^{2+} at the Enzymic Site. Addition of HCO_3^- to enzyme saturated with VO^{2+} did not affect the spectrum for VO^{2+} at the nucleotide site. However, bicarbonate did cause a significant decrease in amplitude of the spectrum for VO^{2+} at the enzymic site, which was accompanied by the appearance of a third spectrum (Figure 5) with distinct *g* values and hyperfine coupling constants (Table 4). This bicarbonate-dependent spectrum could actually be seen in some samples prior to the addition of bicarbonate and may have been caused by bicarbonate in equilibrium with CO_2 in solution. The concentration of HCO_3^- in solution at physiological pH and temperature is 0.2 mM (Butler, 1982), and since the K_m for this substrate is 1.6 mM (Barden *et al.*, 1972), this site is partially populated in the absence of added HCO_3^-, particularly in the presence of activating monovalent cations (Figure 5B). The bicarbonate-dependent spectrum was simulated with *g* values and hyperfine coupling constants (Table 4) that were similar to those for the enzymic site. The decrease of 4×10^{-4} cm^{-1} in $A\|$ for VO^{2+} at the enzymic site that accompanies bicarbonate binding is consistent with the substitution of a neutral oxygen ligand, such as a water molecule or an alcohol, with an anionic oxygen ligand of bicarbonate (Chasteen, 1981; Lord & Reed, 1990). The decrease in $A\|$ gives evidence for the replacement of a water ligand with a bicarbonate oxygen ligand, but it does not rule out the possibility that a bicarbonate-induced conformational change affects the first coordination sphere of the enzymic vanadyl cation to cause the observed change in coupling constant. This effect of bicarbonate on the EPR spectrum was observed prior to and after population of the nucleotide binding site with ADP, ATP, γ-F-ATP, or γ-S-ATP, providing evidence for random binding of ATP and bicarbonate, and for the existence of an enzyme−ADP−HCO_3^- dead-end complex (Barden *et al.*, 1972). Monovalent cation

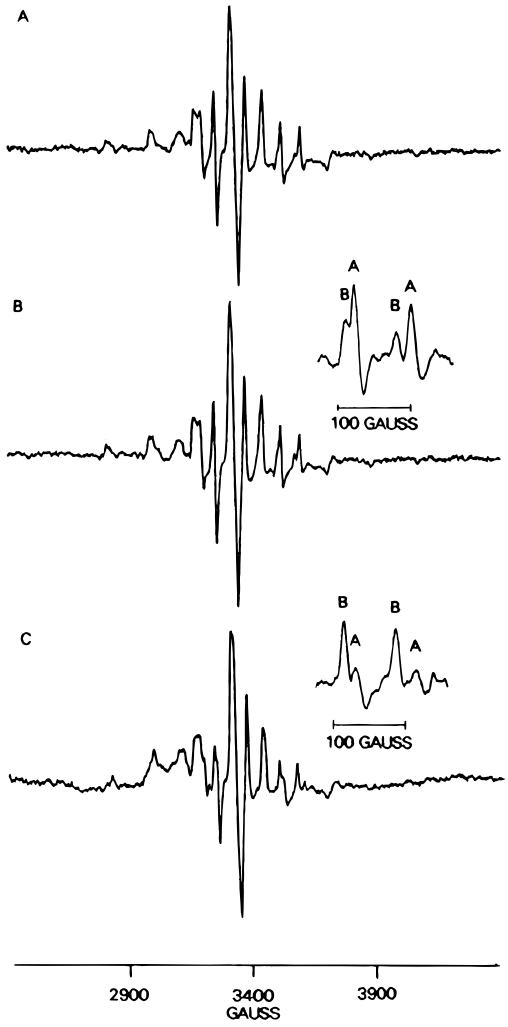

FIGURE 5: Effects of bicarbonate on the spectra for the enzyme−VO^{2+} complexes. The enzyme was prepared by dialysis against 100 mM Hepes−$(CH_3)_4NOH$ at pH 7.8, 6% glycerol, and 1 mM dithioerythritol. EPR spectra were recorded at 9.4 GHz and 273 K with a modulation amplitude of 6.3 gauss. EPR sample A contained 850 μM enzyme subunit, 1.58 mM tetramethylammonium CoASAc, and 2 mM $VOSO_4$. Sample B contained 830 μM enzyme subunit, 1.56 mM tetramethylammonium CoASAc, 1.97 mM $VOSO_4$, and 4.92 mM $TlNO_3$. Sample C contained 810 μM enzyme subunit, 1.51 mM tetramethylammonium CoASAc, 1.91 mM $VOSO_4$, 4.76 mM $TlNO_3$, and 31.7 mM tetramethylammonium bicarbonate. Transition peaks designated by A are produced by the VO^{2+}−enzyme complex. Those designated by B are maximized when bicarbonate is added.

activator and the essential cofactor, CoASAc, were not required for the bicarbonate-dependent change in coupling constant.

Carbamoyl phosphate, an analogue of the putative carboxyphosphate intermediate, affected the equilibrium between the VO^{2+}−enzyme and VO^{2+}−enzyme−HCO_3^- species. Upon addition of $NH_2COPO_4^{2-}$ to the VO^{2+}−enzyme−HCO_3^- complex (Figure 5), the spectrum for the VO^{2+}−enzyme complex was restored as the predominant species. The amplitude of the signal for the enzyme−VO^{2+} complex increased by a factor of 2, while the amplitude of the bicarbonate-dependent spectrum decreased by a factor of 2 (data not shown). The observed effect on the equilibrium between the two spectra is most likely due to displacement of HCO_3^-, a putative ligand of the enzymic divalent cation, from its binding site by carbamoyl phosphate. While carbamoyl phosphate appears to displace bicarbonate, no

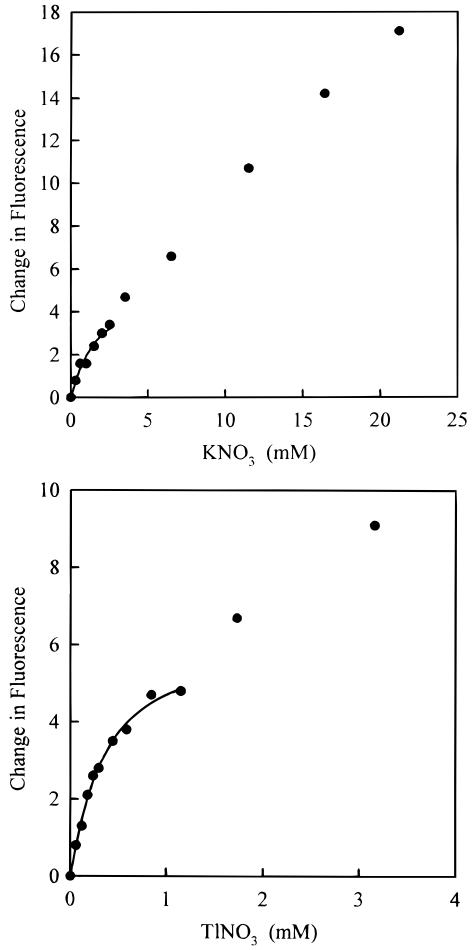

FIGURE 6: Quenching of intrinsic protein fluorescence by monovalent cations. The enzyme samples contained 4 μM enzyme subunit and 130 μM CoASAc in 100 mM Hepes−$(CH_3)_4NOH$ at pH 7.8, 6% glycerol, and 1 mM β-mercaptoethanol. Intrinsic protein fluorescence was monitored at 337 nm (excitation maximum = 294 nm) as the samples were titrated with KNO_3 and $TlNO_3$. The absolute decrease in fluorescence, or quench, is plotted *versus* monovalent cation concentration. The solid lines are the fit of the data to eq 3. A 3 nm red shift of the emission maximum was observed beyond the first phase of the titration. These data points, for which the emission maximum was shifted, were not fit to eq 3.

evidence in the form of a new spectrum was observed for a carbamoyl phosphate ligand to VO^{2+} at the enzymic site. The spectral parameters for VO^{2+} bound at either the enzymic or nucleotide sites were not affected by the CoASAc activator or the substrates, phosphate, and pyruvate.

Monovalent Cation Activation of Pyruvate Carboxylase. Monovalent cations from group 1A and thallium provide 3−7 fold activation of pyruvate carboxylase activity (Barden & Scrutton, 1974). We observed that potassium and thallium yielded 1.9 and 2.3 fold activation, respectively, of enzyme activity in the forward direction in a reaction mixture containing no additional monovalent cation other than $(CH_3)_4N^+$. Tetramethylammonium nitrate was added to maintain a constant ionic strength during the titrations. The activator constants, K_a, for potassium and thallium were 1.2 $\pm$ 0.4 mM and 0.3 $\pm$ 0.1 mM, respectively (data not shown).

Intrinsic Protein Fluorescence Quenching by the Monovalent Cations. Binding of potassium and thallium was monitored by the quenching of intrinsic protein fluorescence upon titration with KNO_3 and $TlNO_3$ (Figure 6). Both titration curves were biphasic, with a 3 nm red shift

accompanying the second phase at excess monovalent cation concentrations. This red shift could possibly be due to a decrease in the hydrophobicity of the environment of the chromophore(s) caused by a metal ion induced conformational change. A K_d of 1.5 ± 0.1 mM for an enzyme−potassium complex was obtained by fitting the first phase of the titration curve to the Hill equation (eq 3), $n_{app} = 1.1 \pm 0.2$. The first phase of the Tl^+ titration curve was also fit to eq 3, yielding a K_d of 0.33 ± 0.06 mM and n_{app} of 1.1 ± 0.1. Excellent agreement between the dissociation constants and the activator constants described above suggests that the monovalent site (or sites) observed by fluorescence quenching is responsible for activation of pyruvate carboxylase. It is possible that the monovalent cation activator site is in the vicinity of the enzymic divalent cation site, since saturation of either site resulted in fluorescence quenching. Population of the two sites could affect the same chromophore (or chromophores) at the first subsite. HCO_3^- enhanced the affinity of the enzyme for Tl^+ by a factor of 2, suggesting that the substrate and monovalent cofactor may interact with each other at the first subsite. In the presence of 20 mM HCO_3^-, the K_d of the Tl^+−enzyme complex was determined to be 160 ± 20 μM ($n_{app} = 1.20 \pm 0.11$) upon quenching of intrinsic protein fluorescence.

Effects of Tl^+ on the VO^{2+} EPR Spectra. Thallous ion was used as a probe of the monovalent cation binding site(s) in VO^{2+} EPR experiments. Superhyperfine coupling between the electron spin of VO^{2+} and the nuclear spin of thallium ($I = {}^1/_2$) can be observed if the two metal ions share a common first coordination ligand or are close enough for direct orbital overlap (Lord & Reed, 1987; Markham & Leyh, 1987). Such coupling, if resolved, would result in splitting of each VO^{2+} EPR signal into a doublet. No superhyperfine coupling was observed upon addition of 5 mM thallium nitrate (enough to saturate the monovalent cation activator site) to the VO^{2+}−enzyme, VO^{2+}−enzyme−HCO_3^-, or VO^{2+}−nucleotide−enzyme complexes. Therefore, the monovalent cation (or cations) that is required for maximal activity at pH 7.8 is unlikely to share a ligand with either the enzymic or the nucleotide VO^{2+} cation. However, when the thallous ion concentration was increased to 30−40 mM, through bond coupling between Tl^+ nuclear spin and ^{51}V electron spin in the $VOADP^-$−enzyme (Figures 7 and 8) and the $VOATP^{2-}$−enzyme species was resolved. The superhyperfine coupling constants measured from solution spectra were $A\| = 33 \times 10^{-4}$ cm^{-1} and $A\perp = 33 \times 10^{-4}$ cm^{-1} for the ADP complex, and $A\| = 33 \times 10^{-4}$ cm^{-1} and $A\perp = 33 \times 10^{-4}$ cm^{-1} for the ATP complex. Superhyperfine coupling between VO^{2+} of the $VOADP^-$−enzyme complex and thallium was well resolved upon freezing of the sample, permitting simulation of the spectrum with parallel and perpendicular superhyperfine constants of 33.4×10^{-4} cm^{-1} (Figure 8). Through bond coupling indicates that thallous ion at an additional monovalent site shares a ligand with VO^{2+} at the nucleotide binding site.

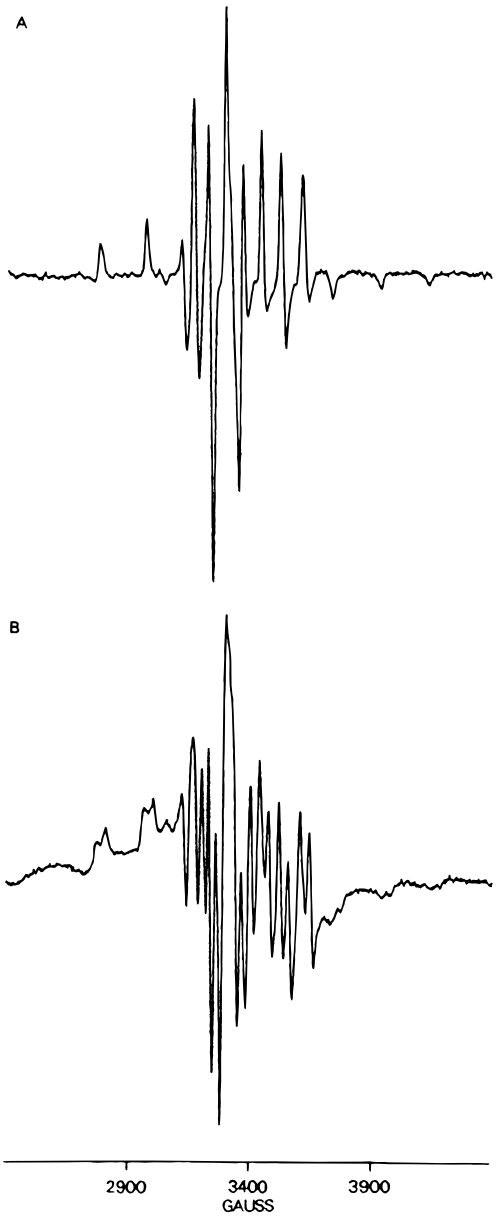

FIGURE 7: Superhyperfine coupling between Tl^+ nuclear spin and the electron spin of VO^{2+} at the nucleotide binding site. EPR spectra were recorded at 9.4 GHz. The enzyme was prepared by dialysis against 100 mM Hepes−$(CH_3)_4NOH$ at pH 7.8, 6% glycerol, and 1 mM dithioerythritol. Spectrum A was recorded at 273 K with a modulation amplitude of 6.3 gauss from a sample that contained 690 μM enzyme subunit, 2.0 mM $VOSO_4$, 1.2 mM tetramethylammonium CoASAc, and 4 mM tetramethylammonium ADP. The VO^{2+}−enzyme spectrum was subtracted from spectrum A. Spectrum B was recorded at 200 K from a sample that contained 830 μM enzyme subunit, 1.7 mM $VOSO_4$, 1.1 mM tetramethylammonium CoASAc, 3.6 mM tetramethylammonium ADP, and 34 mM $TlNO_3$; this sample was frozen to improve resolution of the superhyperfine coupling. The VO^{2+}−enzyme spectrum was subtracted from spectrum B.

DISCUSSION

The rate of oxaloacetate decarboxylation uncoupled from ATP formation was stimulated in the presence of VO^{2+}, $VOADP^-$, P_i, and CoASAc. In the presence of these cofactors, the carboxyl group removed from oxaloacetate may be released in subsite 1, subsite 2, or between the subsites. CO_2 is most probably not released outside the two subsites, because CO_2-biotin is a stable intermediate in the absence of substrates and substrate analogues with a reported half-life of 342 min at 0 °C (Attwood & Wallace, 1986). The lack of significant substrate inhibition of this activity by oxaloacetate suggests that CO_2-biotin is also not decarboxylated to a significant extent in subsite 2. Significant substrate inhibition by oxaloacetate would be expected if the sites for CO_2-biotin and oxaloacetate in subsite 2 overlap, and if CO_2-biotin must reside in subsite 2 during the VO^{2+}, $VOADP^-$, P_i, and CoASAc-induced decarboxylation. How-

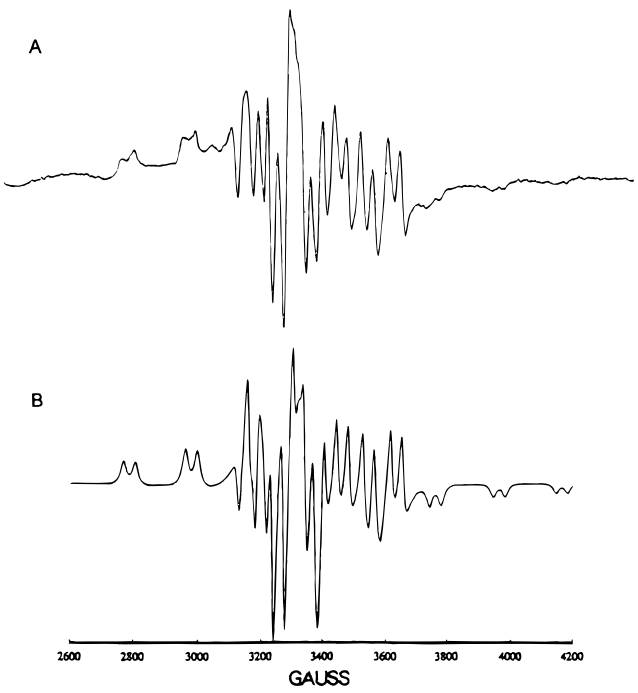

FIGURE 8: Simulation of superhyperfine coupling at the nucleotide site. Spectrum B is a simulation of spectrum A, which is identical to spectrum B in Figure 7, generated by QPOW (Nilges, 1979; Belford and Nilges, 1979; and Maurice, 1982) with the parameters reported in Table 4 and a superhyperfine coupling constant of 33.4 $\times$ 10^{-4} cm^{-1}.

ever, such an effect was not observed. By comparison, oxaloacetate is a substrate inhibitor of the oxamate-induced decarboxylation of oxaloacetate at subsite 2, with a $K_i = 95$ μM (Attwood & Cleland, 1986). Inhibition by oxaloacetate of this activity is thought to result from competition between oxamate and oxaloacetate or between CO_2-biotin and oxaloacetate for subsite 2.

The enhancement of the rate of oxaloacetate decarboxylation by substrates and cofactors that bind in subsite 1 (VO^{2+}, $VOADP^-$ and P_i) is indirect evidence that CO_2-biotin is decarboxylated in this subsite. The effects of bicarbonate, another substrate that binds in subsite 1, on the EPR parameters of the enzymic VO^{2+} cation suggest that the enzymic divalent cation site is located within subsite 1 where $VOADP^-$ and P_i bind. The binding of VO^{2+}, $VOADP^-$, and P_i at the first subsite most likely induces the decarboxylation of CO_2-biotin at subsite 1. The location of the binding site for CoASAc, the fourth component required for the induction of oxaloacetate decarboxylation remains unknown, but CoASAc may also bind in subsite 1. This study has provided the first evidence suggesting that CO_2-biotin is labile in subsite 1 in the presence of cofactors and substrates.

The release of CO_2 in subsite 1 in the presence of VO^{2+}, $VOADP^-$, and P_i and in subsite 2 in the presence of oxamate (Attwood & Cleland, 1986) suggests that CO_2 is not released from carboxybiotin in either subsite until substrates or acceptors are bound. The acceptors may cause conformational changes that enhance the affinity of CO_2-biotin for the subsites where it is labile, or they may cause conformational changes within the subsites that promote the release of CO_2 from CO_2-biotin. HCO_3^- and ATP did not enhance the rate of oxaloacetate decarboxylation, suggesting that they do not induce the release of CO_2 from CO_2-biotin. Rather, $MgATP^{2-}$ and Mg^{2+} actually increase the half-life of the CO_2-biotin intermediate (Attwood & Graneri, 1992). Induction of the decarboxylation of CO_2-biotin by substrates is essential for efficient coupling of the partial reactions of this nonclassical ping-pong type mechanism; if carbon dioxide is released at an empty site before the acceptor for the molecule has bound, it can react with water to form bicarbonate resulting in a "hydrolytic leak" (Easterbrook-Smith *et al.*, 1976; Keech & Attwood, 1985; Knowles, 1989). The present results are consistent with a mechanism in which the binding of substrates governs the fate of CO_2-biotin by inducing the release of CO_2.

While VO^{2+} has been useful for uncoupling the partial reactions at the separate subsites of chicken liver pyruvate carboxylase, the inability of VO^{2+} to support catalysis at the first subsite raises concerns about the utility of VO^{2+} as a probe for the divalent cation activator sites. In the presence of VO^{2+}, pyruvate carboxylase cannot catalyze the formation of the putative carboxyphosphate intermediate from phosphate and CO_2, and/or the formation of ATP from carboxyphosphate and ADP in the reverse direction. No phosphate is formed in the presence of pyruvate, bicarbonate, VO^{2+}, and $VOATP^{2-}$, suggesting that carboxyphosphate cannot be formed in the forward direction either. VO^{2+} might not support catalysis at subsite 1 because it might not bind to the same sites as the divalent cation activators Mg^{2+}, Mn^{2+}, and Co^{2+} (Keech & Utter, 1963). Mg^{2+} was only able to displace VO^{2+} from the nucleotide binding site; it could not displace VO^{2+} from the enzymic binding site. However, substantial evidence suggests that VO^{2+} binds to the enzymic and the nucleotide divalent cation activator sites: (i) VO^{2+} and $VOATP^{2-}$ bind randomly to enzymic and nucleotide divalent sites as do Mg^{2+} and $MgATP^{2-}$ (Barden & Scrutton, 1974); (ii) VO^{2+} and Mg^{2+} compete with each other for the nucleotide divalent cation binding site; (iii) VO^{2+} binding to an enzymic divalent site results in quenching of intrinsic protein fluorescence as does the binding of Mg^{2+} and Mn^{2+}; (iv) $VOATP^{2-}$ and bicarbonate bind randomly to pyruvate carboxylase as do $MgATP^{2-}$ and bicarbonate (Barden *et al*., 1972); (v) $VOADP^-$ and bicarbonate bind simultaneously as do $MgADP^-$ and bicarbonate (Barden *et al*., 1972). Thus, VO^{2+} appears to be a good probe of the divalent cation sites in subsite 1.

In addition to inducing the decarboxylation of CO_2-biotin at the first subsite, a second role for the enzymic divalent cation could be to orient bicarbonate for attack on the γ-phosphoryl group of ATP during the carboxylation of pyruvate. The effect of bicarbonate on the EPR properties of the enzymic vanadyl cation strongly suggests that bicarbonate is a first coordination sphere ligand to VO^{2+}. A third role for the metal could be to minimize charge repulsion between anionic species during the attack of bicarbonate on ATP. There are other plausible roles for the nucleotide bound divalent cation as well; it may (i) neutralize the negative charge of ATP, (ii) orient ATP properly for the impending nucleophilic attack by bicarbonate, (iii) enhance the electrophilic nature of phosphorus at the γ position, and (iv) make ADP a better leaving group in the formation of carboxyphosphate.

Evidence for at least one monovalent cation activator site in the first subsite was observed by fluorescence quenching. The monovalent site may be near the enzymic divalent site, where binding of M^{2+} also results in fluorescence quenching. Tighter binding of the monovalent cation observed in the

presence of bicarbonate suggests that the monovalent activator binds in the vicinity of bicarbonate and that there may be an interaction between the substrate and activator. The EPR results indicate that bicarbonate can bind before monovalent cation, in agreement with the steady-state kinetic results indicating that bicarbonate binds before K^+ (Barden & Scrutton, 1974). Similar to the role postulated for the enzyme bound divalent cation, the monovalent activator may neutralize the negative charge of bicarbonate to minimize charge repulsion when bicarbonate attacks the γ-phosphoryl group ATP.

Through bond superhyperfine coupling between the nuclear spin of Tl^+ and the electron spin of ^{51}V of $VOATP^{2-}$ and $VOADP^-$ provides direct evidence for a common ligand shared by vanadyl at the nucleotide site and Tl^+ at a second monovalent cation site (Markham & Leyh, 1987; Lord & Reed, 1987). At the higher monovalent cation concentrations, the cation probably forms a complex with the nucleotide itself either before or after the nucleotide site on the enzyme is populated. Saturation of this second monovalent site did not further activate the enzyme, indicating that this is not an essential monovalent site. However, monovalent cation binding at this site could possibly be involved in catalysis at higher pH. At pH 9.5, the rate of catalysis in the absence of CoASAc is enhanced by 60 mM potassium to a level that is 2% of the CoASAc-dependent rate at pH 7.8 (Phillips *et al*., 1992). The monovalent cation that shares an ATP ligand with VO^{2+} could be responsible for the observed activation. K^+ could facilitate the nucleophilic reaction between bicarbonate and $VOATP^{2-}$ by neutralizing the negative charge of ATP, but as of yet there is no evidence to suggest that the second monovalent cation site observed by EPR is the CoASAc-independent activator site.

CONCLUSIONS

VO^{2+} EPR experiments have provided evidence that 2 equiv of divalent cation bind at subsite 1 of pyruvate carboxylase. Bicarbonate is thought to bind to the enzymic VO^{2+}, while a second VO^{2+} is involved in nucleotide substrate binding. Kinetic studies in the presence of VO^{2+} indicate that the decarboxylation of oxaloacetate at subsite 2 is uncoupled from ATP formation at subsite 1, and that the release of CO_2 from carboxybiotin is induced by the binding of substrates at subsite 1. Pyruvate carboxylase essentially becomes an oxaloacetate decarboxylase in the presence of VO^{2+}, as it is able to effectively catalyze the decarboxylation of oxaloacetate in the absence of the complete forward or reverse pyruvate carboxylase reactions.

ACKNOWLEDGMENT

We thank Dr. George D. Markham of the Fox Chase Institute for Cancer Research for his advice and technical assistance. QPOW EPR simulation software was furnished by Dr. R. Lynn Belford of the Illinois ESR Research Center, supported by NIH RR01811.

REFERENCES

Albanese, N. F., & Chasteen, N. D. (1978) *J. Phys. Chem. 82*, 910−914.
Attwood, P. V. (1993) *Biochemistry 32*, 12736−12742.
Attwood, P. V., & Cleland, W. W. (1986) *Biochemistry 25*, 8191−8196.
Attwood, P. V., & Graneri, B. D. L. A. (1991) *Biochemical J. 273*, 443−448.
Attwood, P. V., & Graneri, B. D. L. A. (1992) *Biochemical J. 287*, 1011−1017.
Attwood, P. V., Tipton, P. A., & Cleland, W. W. (1986) *Biochemistry 25*, 8197−8205.
Attwood, P. V., & Wallace, J. C. (1986) *Biochem. J. 235*, 359−364.
Barden, R. E., Fung, C. -H., Utter, M. F., & Scrutton, M. C. (1972) *J. Biol. Chem. 247*, 1323−1333.
Barden, R. E., & Scrutton, M. C. (1974) *J. Biol. Chem. 249*, 4829−4838.
Belford, R. L., & Nilges, M. J. (1979) *Computer Simulation of Powder Spectra*. Presented at EPR Symposium, 21st Rocky Mountain Conference; Denver, CO.
Butler, J. N. (1982) *Carbon Dioxide Equilibria and Their Applications*, pp 259, Addison-Wesley, Reading, MA.
Carver, J. A., Baldwin, G. S., Keech, D. B., Bais, R., & Wallace, J. C. (1988) *Biochemical J.* 252, 501−507.
Chasteen, N. D. (1981) in *Biological Magnetic Resonance* (Berliner, L. J., & Reuben, J., Eds.) pp 53−119, Plenum Press, New York.
Cleland, W. W. (1970) in *The Enzymes, Vol. 2, 3rd ed.* (Boyer, P., Ed.) p 1, CRC Press, Boca Raton.
Duggelby, R. G., Attwood, P. V., Wallace, J. G., & Keech, D. B. (1982) *Biochemistry 21*, 3364−3370.
Easterbrook-Smith, S. B., Hudson, P. J., Goss, N. H., Keech, D. B., & Wallace, J. C. (1976) *Arch. Biochem. Biophys. 176*, 709−720.
Fitzgerald, J. J., & Chasteen, N. D. (1974) *Anal. Biochem. 60*, 170−180.
González-Romo, P., Sánchez-Nieto, S., & Gavilanes-Ruíz, M. (1992) *Anal. Biochem. 200*, 235−238.
Goodall, G. J., Baldwin, G. S., Wallace, J. C., & Keech, D. B. (1981) *Biochemical J. 199*, 603−609.
Keech, D. B., & Attwood, P. V. (1985) in *Pyruvate carboxylase* (Keech, D., & and Wallace, J. C., Eds.), CRC Press, Boca Raton.
Keech, D. B., & Utter, M. F. (1963) *J. Biol. Chem. 238*, 2609−2614.
Knowles, J. R. (1989) *Annu. Rev. Biochem. 58*, 195−221.
Lord, K. A., & Reed, G. H. (1987) *Inorg. Chem. 26*, 1464−1466.
Lord, K. A., & Reed, G. H. (1990) *Arch. Bioch. Biophys. 281*, 124−131.
Markham, G. D. (1984) *Biochemistry 23*, 470−478.
Markham. G. D., & Leyh, T. S. (1987) *J. Am. Chem. Soc. 109*, 599−600.
Maurice, A. M. (1982) Ph.D. Thesis, University of Illinois, Urbana, Illinois.
McClure, W. R., Lardy, H. A., & Kneifel, P. H. (1971a) *J. Biol. Chem. 246*, 3569−3578.
McClure, W. R., Lardy, H. A., Wagner, M., & Cleland W. W. (1971b) *J. Biol. Chem. 246*, 3579−3583.
Mustafi, D., Telser, J., & Makinen, M. W. (1992) *J. Am. Chem. Soc. 114*, 6219−6226.
Nilges, M. J. (1979) Ph.D. Thesis, University of Illinois, Urbana, Illinois.
Phillips, N. F. B., Snoswell, M. A., Chapman-Smith, A., Keech, D. B., & Wallace, J. C. (1992) *Biochemistry 31*, 9445−9450.
Reed, G. H., & Scrutton, M. C. (1974) *J. Biol. Chem. 249*, 6156−6162.
Scrutton, M. C., & Fung, C.-H. (1972) *Arch. Biochem. Biophys. 150*, 636−647.
Scrutton, M. C., Keech, D. B., & Utter, M. F. (1965) *J. Biol. Chem. 240*, 574−581.
Scrutton, M. C., Utter, M. F., & Mildvan, A. S. (1966) *J. Biol. Chem. 241*, 3480−3487.
Segel, I. H. (1975) *Enzyme Kinetics*, pp 360−361, John Wiley & Sons, New York.
Wallace, J. C., Phillips, N. F. B., Snoswell, M. A., Goodall, G. J., Attwood, P. V., & Keech, D. B. (1985) *Ann. N. Y. Acad. Sci. 447*, 169−188.
Werneburg, B. G., & Ash, D. E. (1993) *Arch. Biochem. Biophys. 303*, 214−221.
Zhang, C., Markham, G. D., & LoBrutto, R. (1993) *Biochemistry 32*, 9866−9873.

BI971282R